Cobrotoxin Inhibits NF-κB Activation and Target Gene Expression through Reaction with NF-κB Signal Molecules

Mi Hee Park,[‡] Ho Seub Song, [§] Ki Hyun Kim,[§] Dong Ju Son,[‡] Seung Ho Lee,[‡] Do Young Yoon,[||] Youngsoo Kim,[‡] Il Young Park,[‡] Sukgil Song,[‡] Bang Yeon Hwang,[‡] Jae Kyung Jung,[‡] and Jin Tae Hong*[,‡]

College of Pharmacy, Chungbuk National University, 48, Gaesin-dong, Heungduk-gu, Cheongju, Chungbuk 361-763, Korea, College of Oriental Medicine, Kyungwon University 65, Bukjeong-Dong, Sujeong-gu, Seongnam, Gyeonggii 461-701, Korea, and Korea Research Institute of Bioscience and Biotechnology, 52, Oun-dong, Yusong-gu, Taejon, 305-333, Korea

Received January 27, 2005; Revised Manuscript Received April 19, 2005

ABSTRACT: Cobrotoxin is known to bind with cysteine residues of biological molecules such as nicotine acetylcholine receptor. Cobrotoxin may modify IKKs and p50 through protein−protein interaction since cysteine residues are present in the kinase domains of IKKα and IKKβ and in the p50 of NF-κB. Our surface plasmon resonance analysis showed that cobrotoxin directly binds to p50 ($K_d = 1.54 \times 10^{-5}$ M), IKKα ($K_d = 3.94 \times 10^{-9}$ M) and IKKβ ($K_d = 3.4 \times 10^{-8}$ M) with high binding affinity. Moreover, these protein−protein interactions suppressed the lipopolysaccharide (LPS, 1 μg/mL)- and the sodium nitroprusside (SNP, 200 μM)-induced DNA binding activity of NF-κB and NF-κB-dependent luciferase activity in astrocytes and Raw 264.7 macrophages. These inhibitory effects were correlated with the inhibition of IκB release and p50 translocation. Inhibition of NF-κB by cobrotoxin resulted in reductions in the LPS-induced expressions of COX-2, iNOS, $cPLA_2$, IL-4, and TNF-α in astrocytes and in COX-2 expression induced by SNP, LPS, and TNF-α in astrocytes. Moreover, these inhibitory effects of cobrotoxin were reversed by adding reducing agents, dithiothreitol and glutathione. In addition, cobrotoxin did not have any inhibitory effect on NF-κB activity in cells carrying mutant p50 (C62S), IKKα (C178A), and IKKβ (C179A), with the exception of IKKβ (K44A) mutant plasmid. Confocal microscopic analysis showed that cobrotoxin is uptaken into the nucleus of cells. These results demonstrate that cobrotoxin directly binds to the sulfhydryl groups of p50 and IKKs, and that this results in reduced IκB release and the translocation of p50, thereby inhibiting the activation of NF-κB.

Nuclear factor kappa B (NF-κB) is one of the most important transcription factors and regulates various immediate cellular genes involved in immune and acute phase, inflammatory responses and in cell survival (*1*, *2*). NF-κB is located in the cytoplasm of nonstimulated cells by an interaction with inhibitory proteins, such as IκBs, but responds to proinflammatory stimuli, when IκBs are rapidly phosphorylated and degraded, which results in the release of free NF-κB dimmers (p50 and Rel A) that translocate to the nucleus for the transcription of target genes. IκB kinase (IKK) is the protein kinase responsible for IκB phosphorylation and degradation in response to proinflammatory stimuli (*3*, *4*). Structurally, IKK subunits have cysteine residues in the kinase domain of IKKα (Cys-178) and IKKβ, and some of these are located at functionally important sites (Cys-179), such as at the activating T loop and at the catalytic site (*5*, *6*). The p50 subunit also possesses a critical cysteine residue (Cys-62) in the N-terminal region of its DNA-binding domain (*7*−*9*). In several studies, potent inhibitors of NF-κB activation have been shown to interact with specific cysteine residues of the IKK catalytic subunits or p50 subunit of NF-κB, and this results in the targeted inactivation of NF-κB (*5*−*7*). Moreover, this interaction was found to be reversed by thiol-modifying agents, and the expressions of mutant IKKα, IKKβ, and p50, in which cysteine residues were replaced with other amino acids (alanine (IKK) or serine (p50)) rendered the cells resistant to the inhibitory effects of these inhibitors on NF-κB activation (*5*−*7*), which suggests that cysteines in proteins involving NF-κB signaling may be targets of these compounds.

Currently, the elucidations of important molecular interfaces of specific toxin-receptor/ion channel complexes have been largely studied as a result of drug discovery initiatives (*10*−*14*). Cobrotoxin, a snake venom toxin of *Vipera lebetina turanica*, is actually a group of basic peptides composed of 235 amino acids with six disulfide bonds formed by 12 cysteines (*14*, *15*). And, it has been reported that long-chain snake toxin possessing five disulfide bonds has higher affinity for the nicotinic acetylcholine receptor (AchR) ($K_d = (1\sim12) \times 10^{-9}$ M) than short-chain snake toxins with four disulfide bonds ($K_d = (3\sim22) \times 10^{-6}$ M), and that reducing the 5th disulfide bond lowers binding affinity to AchR ($K_d = 12 \times 10^{-6}$ M) (*16*). Michalet et al. reported that the Cys192−193 residues of αγ subunit of AchR are a binding target of snake toxin, and that the disulfide bond of snake toxin may be core or additional specific binding amino acid residues (*17*−*20*).

* Address all correspondence to Dr. Jin Tae Hong, College of Pharmacy, Chungbuk National University 48, Gaesin-dong, Heungduk-gu, Cheongju, Chungbuk, 361-763, Korea. Phone, 82-43-261−2813; fax, 82-43-268-2732; e-mail, jinthong@cbucc.chungbuk.ac.kr.

[‡] Chungbuk National University.

[§] Kyungwon University.

[||] Korea Research Institute of Bioscience and Biotechnology.

10.1021/bi050156h CCC: $30.25
Published on Web 05/18/2005

These data suggest that cobrotoxin can bind to other molecular targets possessing sulfhydryl groups and thus alter the biological activities of these molecules. We previously found that melittin and bee venom toxin interact with the p50 subunit of NF-κB, and thereby reduce its activity (*21*). In the present study, we investigated whether cobrotoxin may bind to the sulfhydryl groups of p50 and of IKKs to inhibit NF-κB activity and its target gene expression in the Raw 264.7 cells and astrocytes.

EXPERIMENTAL PROCEDURES

Chemicals. The expression plasmid encoding IKKβK44A-Flag was obtained from Dr. Warner C. Greene (University of California, San Francisco, CA) (Lin et al., 2000), and the expression plasmid encoding IKKαC178A-Flag and IKKβC179A-Flag was obtained from Dr. Dae-Myung Jue (University of Catholic, Seoul, South Korea) (Jeon et al., 2000 (*27*)). Rabbit polyclonal antibodies to p50 (1:500), p65 (1:500), IκB (1:500), phosphorylated IκB (1:500), and cPLA2 (dilution 1:500), goat polyclonal antibody to COX-2 (1:500) and TNF-α (1:500), mouse polyclonal antibody to iNOS (1:500) and IL-4 (1:500), and all of the secondary antibodies used in Western blot analysis were purchased from Santa Cruz Biotechnology (Santa Cruz, CA). T4 polynucleotide kinase was obtained from Promega (Madison, WI). Poly (dI·dC), horseradish peroxidase-labeled donkey anti-rabbit second antibody and the ECL detection reagent were obtained from Amersham Pharmacia Biotech (Centennial Ave., NJ). Reagents for SDS−polyacrylamide gel electrophoresis were from Bio-Rad (Hercules, CA). LPS, monoclonal anti-β-actin antibody, and WST-1 were purchased from Sigma-Aldrich (St. Louis, MO). All other reagents were also purchased from Sigma-Aldrich unless otherwise stated. Cobrotoxin was purchased from Sigma-Aldrich and its composition was as follows: protein (90 ± 2%), phospholipase A2 (35 ± 6 U), coagulase (80 000 ± 80 00 U/mg).

Raw 264.7 Cell Culture. Raw 264.7 cells, a mouse macrophage-like cell line, were obtained from the American Type Culture Collection (Cryosite, Lane Cove NSW, Australia). Dulbecco's modified Eagle medium (DMEM), penicillin, streptomycin, and fetal bovine serum were purchased from Gibco Life Technologies (Rockville, MD). Raw 264.7 cells were grown in DMEM containing 10% fetal bovine serum, 100 U/mL penicillin, and 100 μg/mL streptomycin at 37 °C in 5% CO_2-humidified air.

Astrocyte Culture. Sprague−Dawley rats were maintained in accordance with the policy of the National Institute of Toxicological Research, which is also in line with the Korea Food and Drug Administration's guidelines on the care and use of laboratory animals. Sprague−Dawley rats weighing 200−300 g were housed under a 12 h light/dark cycle, at 23 °C and 60 ± 5% humidity. All animals had free access to food (Samyang Foods, Co., Seoul, Korea) and water. Cerebral cortical cells were isolated from neonatal rat brain (day 1) in phosphate-buffered saline (pH 7.6). After washing with Dulbecco's modified Eagle's medium (DMEM), isolated cells were incubated for 15 min in DMEM containing 0.2% trypsin. Cells were then dissociated by trituration and plated into polyethyleneimine-coated culture dishes (5×10^6 cells/60 cm dish) containing minimum essential medium and Eagle's salts supplemented with 5% heat-inactivated fetal bovine serum, 2 mM L-glutamine, 1 mM pyruvate, 20 mM KCl, 10 mM sodium bicarbonate, and 1 mM Hepes (pH 7.2). After 3 days in culture, the culture medium was replaced with DMEM containing 5% fetal bovine serum, and repeated every 3 days. Cells were cultured for designated times. Cultured cells contained <10% neuronal cells. Cells grown on LabTek chamber slides (Nalge Nunc International, NY) were used for immunochemical studies.

Cell Viability Assay. Cell viability was determined using the WST-1 assay (Dojin Laboratory, Kumamoto, Japan) according to the manufacturer's instructions. WST-1 solution was added to cells in 96-well plates; cells were then incubated at 37.5 °C for 1 h, and optical densities of wells were read at 450 nm.

Western Blot Analysis. Cells were homogenized with lysis buffer [50 mM Tris, pH 8.0, 150 mM NaCl, 0.02% sodium azide, 0.2% SDS, 1 mM PMFS, 10 μL/mL aprotinin, 1% igapel 630 (Sigma-Aldrich, St. Louis, MO), 10 mM NaF, 0.5 mM EDTA, 0.1 mM EGTA, and 0.5% sodium deoxycholate] and centrifuged at 23 000*g* for 1 h. Equal amount of proteins (80 μg) were then separated on a SDS/12%-polyacrylamide gel, and transferred to nitrocellulose membrane (Hybond ECL, Amersham Pharmacia Biotech Inc., Piscataway, NJ). Blots were blocked for 2 h at room temperature with 5% (w/v) nonfat dried milk in Tris-buffered saline [10 mM Tris (pH 8.0) and 150 mM NaCl] solution containing 0.05% Tween-20. Membranes were incubated for 5 h at room temperature with specific antibodies, that is, goat polyclonal p65, COX-2, TNF-α, and p50 antibody (1:1000), IκB (1:500), phosphorylated IκB (1:500) and cPLA2 (1:500), and mouse monoclonal iNOS and IL-4 antibodies (1:500) (Biotechnology Inc.,Santa Cruz, CA). And, blots were then incubated with the corresponding conjugated anti-rabbit immunoglobulin G-horseradish peroxidase (Biotechnology Inc.,Santa Cruz,CA). Immunoreactive proteins were detected using an ECL western blotting detection system. The relative densities of protein bands were obtained by densitometry using MyImage (SLB, Seoul, Korea) and quantified using Labworks 4.0 software (UVP Inc., Upland, CA).

Nuclear Extracts and EMSA. Gel shift assays were performed according to the manufacturer's recommendations (Promega, Madison, WI). Briefly, 1×10^6 cells/mL was washed twice with 1× PBS; 1 mL of PBS was added, and then the cells were scraped into a cold Eppendorf tube. The cells were spun down at 15 000*g* for 1 min, and the resulting supernatant was removed. Solution A (50 mM Hepes, pH 7.4, 10 mM KCl, 1 mM EDTA, 1 mM EGTA, 1 mM dithiothreitol, 0.1 μg/mL phenylmethylsulfonyl fluoride, 1 μg/mL pepstatin A, 1 μg/mL leupeptin, 10 μg/mL soybean trypsin inhibitor, 10 μg/mL aprotinin, and 0.5% Nonidet P-40) was added to the cell pellets in a 2:1 ratio (v/v) and allowed to incubate on ice for 10 min. Solution C (solution A containing 10% glycerol and 400 mM KCl) was added to the cell pellets in a 2:1 ratio (v/v) and vortexed on ice for 20 min. Cells were centrifuged at 15 000*g* for 7 min, and the resulting nuclear extract supernatant was collected in a chilled Eppendorf tube. Consensus oligonucleotides were end-labeled using T4 polynucleotide kinase and [γ-^{32}P]ATP for 10 min at 37 °C. Gel-shift reactions were assembled and allowed to incubate at room temperature for 10 min; 1 μL (50 000−200 000 cpm) of ^{32}P-labeled oigonucleotide was

then added, and incubation was continued for 20 min at room temperature. For supershift assays, nuclear extracts from cells treated with LPS (1 μg/mL) were incubated with specific antibodies (Abs) against p50, p65, and Rel-A NF-κB isoforms for 1 h before EMSA. For competition assays, nuclear extracts from cells treated with LPS (1 μg/mL) were incubated with unlabeled NF-κB oligonucleotide (50×, 100×, and 200×) or labeled SP-1(100×) and AP-1(100×) for 30 min before EMSA. Subsequently, 1 μL of gel-loading buffer was added to each reaction, loaded onto a 6% nondenaturing gel, and electrophoresed until the dye was three-fourths of the way down the gel. Gel was dried at 80 °C for 1 h and exposed to film overnight at −70 °C. The relative densities of the DNA−protein binding bands were scanned by densitometry using MyImage (SLB, Seoul, Korea) and quantified using Labworks 4.0 software (UVP Inc., Upland, CA).

Transfection and Luciferase Activity Assay. Astrocytes and Raw 264.7 cells were transfected with pNF-κB-Luc plasmid (5× NF-κB; Stratagene, CA) or IKKα (C178A), IKKβ (C179A), and IKKβ (K44A) mutant plasmid using a mixture of plasmid and lipofectAMINE PLUS in the OPTI-MEM kit according to manufacturer's instructions (Invitrogen, Carlsbad, CA). Control pCMV (Clontech, CA) was cotransfected to monitor the transfection efficiencies. After 24 h, the cells were then co-treated with cobrotoxin or LPS, or a combination of LPS and cobrotoxin; luciferase activity was measured using a luciferase assay kit (Promega), according to the manufacturer's instructions (WinGlow, Bad Wildbad, Germany).

Immunofluorescent Labeling and Scanning-Laser Confocal Microscopy. Raw 264.7 cells (0.5×10^6 cells/cm^2) were cultured on a chamber slide (Lab-Tak II chamber slider system, Nalge Nunc Int., Naperville, IL) and treated with LPS with/without cobrotoxin. After 24 h of culture, the cells were fixed in 4% paraformaldehyde, membrane-permeabilized by exposure for 1 h to 0.1% Triton X-100 in phosphate-buffered saline, and placed in blocking serum (5% bovine serum albumin in phosphate-buffered saline) at room temperature. The cells were then exposed to primary goat polyclonal antibody for p50 (1: 100 dilution) overnight at 4 °C. After three washes with ice-cold PBS followed by treatment with an anti-goat biotinylated secondary antibody (Molecular Probes, Eugene, OR) for 1 h at room temperature, immunofluorescence images were acquired using a confocal laser scanning microscope (dual wavelength scan, MRC1024, Bio-Rad, Hercules, CA) equipped a with a 360× oil immersion objective. To determine whether cobrotoxin is uptaken by cells, astrocytes and Raw 264.7 cells (1×10^5 cells/cm^2) were cultured on a chamber slide (Lab-Tak II chamber slider system, Nalge Nunc Int., Napervill, IL) and then treated with cobrotoxin labeled with superior Alexa Fluor 488 dye (Molecular Probe, Eugene, OR). Cells were incubated for 24 h at 37 °C, and then fixed in 4% paraformaldehyde; membranes were permeabilized by exposure for 5 min to 0.2% Triton X-100 in phosphate-buffered saline, and membranes were placed in blocking serum (5% horse or goat serum in phosphate-buffered saline). Immunofluorescence images were acquired using a confocal laser scanning microscope (dual wavelength scan, MRC1024, Bio-Rad, Hercules, CA) with a 60× oil immersion objective.

Surface Plasmon Resonance Analysis. BIACORE 2000 and CM5 sensor chip were both supplied by BIACORE AB (Uppsala, Sweden). Hepes-buffered saline (HBS) buffer, pH 7.4, containing 10 mM Hepes, 1 mM EDTA, 0.001% Tween-20, and 0.15 M NaCl, was used as the constant flow buffer unless otherwise stated. All buffers and solutions used during BIACORE analysis were made up using ultrapure water, degassed, and sterile-filtered. Recombinant protein G and protein p50 were purchased from Sigma-Aldrich (St. Louis, MO). Activated CM-dextran matrix prepared by mixing ethyl-*N*-(dimethylaminopropyl) carbodiimide and *N*-hydroxysuccimide was surfaced on the sensor chip. Recombinant p50 protein or cobrotoxin was then layered onto the CM-dextran sensor chip, and the chip was then blocked using 1 M ethanolamine (pH 8.5). Serial dilutions of cobrotoxin or p50 antibody, and immunoprecipitated IKKα and IKKβ extracted from the nuclear fraction of cells treated with LPS were prepared using Hepes-buffered saline buffer, and then flowed sequentially at increasing concentration. The regeneration of protein interactions were generated by changing of the pH of the solution and then finally determined at pH 12. The BIACORE 2000 system continuously monitors changing mass at the sensor surface, and the kinetics of protein interactions were analyzed using BIAevaluation 3.0 software (BIACORE AB, 5-75450, Uppsala, Sweden).

RESULTS

Cobrotoxin Interacts with p50, IKKα, and IKKβ. To determine whether p50, IKKα, and IKKβ, which have cysteine residue in their active sites, can react with cobrotoxin, surface plasmon resonance analysis was performed. This analysis demonstrated that cobrotoxin binds to the p50 subunit of NF-κB immobilized onto a surface of a sensor chip and that cobrotoxin increased binding activity with p50 in a dose-dependent manner (Figure 1A). The maximum binding affinity (K_d) between cobrotoxin and p50 was 1.54×10^{-5} M in physiological buffer (pH 7.5). We also studied the binding affinity between cobrotoxin and IKKs. Immunoprecipitated IKKs isolated from LPS-stimulated astrocytes were immobilized onto the surface of a sensor chip, and binding affinities were monitored by flowing with several doses of cobrotoxin. The binding affinity between IKKs was found to be much stronger than that between cobrotoxin and p50. The maximum binding affinity between cobrotoxin and IKKα was 2.16×10^{-9}M (K_d) and with IKKβ was 3.24×10^{-8}M (K_d) (Figure 1B,C). Next, we studied the interaction between cobrotoxin immobilized onto a sensor chip and immunoprecipitated p50, IKKα, and IKKβ extracted from nuclear (p50) or cytosolic (IKKα and IKKβ) fractions of cells treated with LPS alone or with LPS and different doses of cobrotoxin. As is shown in Figure 1B, the dose-dependent interaction between cobrotoxin and immunoprecipitated p50, IKKα, or IKKβ extracted from cells treated with LPS and cobrotoxin were much lower than the corresponding interaction with immunoprecipitated p50, IKKα, or IKKβ extracted from the cells treated with LPS alone in dose-dependent manners (Figure 1Ba−c).

Inhibition of NF-κB Activation. One of the consequences of cobrotoxin binding with proteins of the NF-κB signal pathway is the inhibition of IκB release and/or the prevention of p50 translocation to the nucleus, which finally inactivate

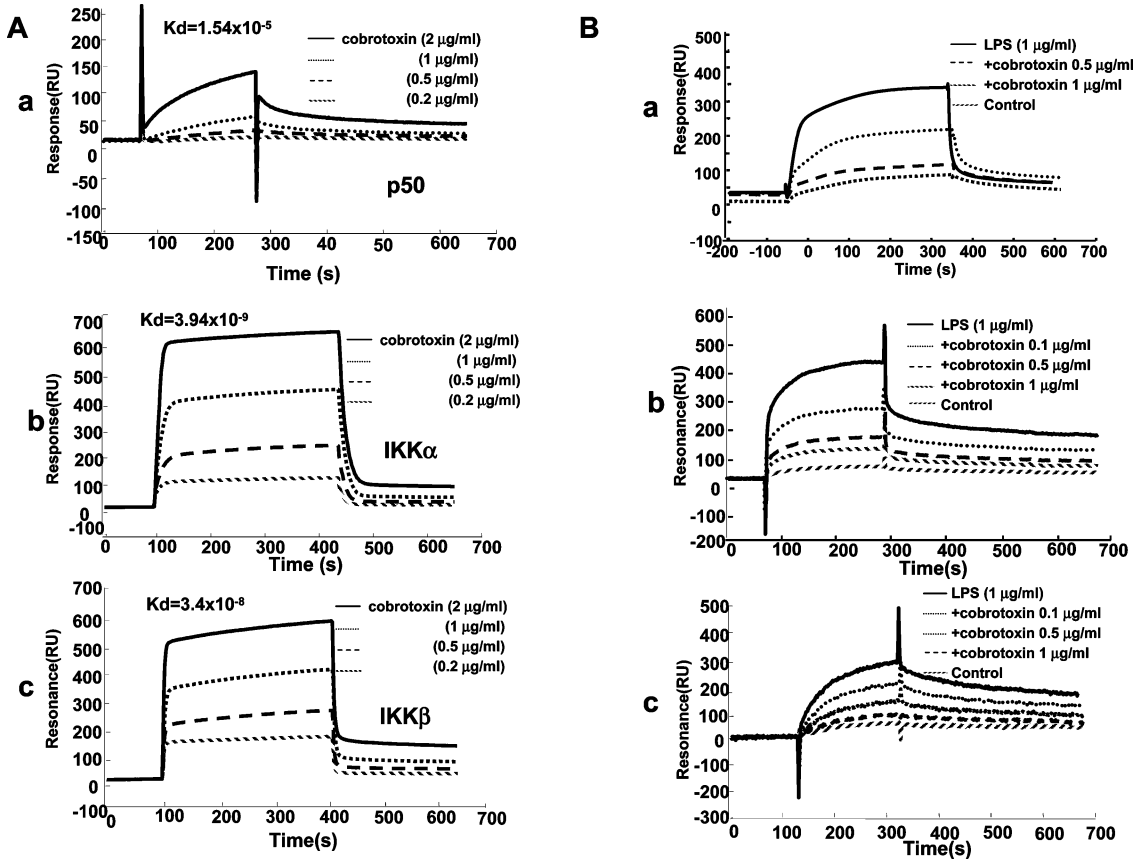

FIGURE 1: Interaction between cobrotoxin and p50 or IKKs. (A and B) Surface plasmon resonance binding kinetic traces of two separate experiments. (Aa) Full kinetic dataset for the binding ability of cobrotoxin to immobilized p50 obtained by immunoprecipitation. (Ab and Ac) Full kinetic dataset for the binding abilities of cobrotoxin to immobilized IKKα and IKKβ obtained by immunoprecipitation to immobilized cobrotoxin. Lines represent fits to a 1:1 binding model at the concentrations indicated. A detail description is included in Materials and Methods. (B) Interactions between cobrotoxin and same amounts (20 μg) of p50 and IKKs. Representative kinetic traces for the interactions between cobrotoxin immobilized onto surface chip and immunoprecipitated p50 (Ba), IKKα (Bb), and IKKβ (Bc), extracted from the nuclear fraction of astrocytes. Lines represent fits to a 1:1 binding kinetic trace. Similar results were obtained from two separate experiments. RU, resonance unit; K_d, binding affinity.

NF-κB DNA binding activity. Therefore, we next studied the consequence of the interaction between molecules of NF-κB signal and associated species and cobrotoxin. Protein p50 was incubated with the NF-κB DNA binding element in the absence or presence of cobrotoxin in vitro, and then EMSA was performed to determine the binding ability between the two. The inhibitory effect of cobrotoxin (0.1−1 μg/mL) on the binding between p50 and the NF-κB binding element was observed (Figure 2A). NF-κB DNA binding activity was then examined by EMSA in nuclear extracts of astrocytes treated with LPS alone, or LPS in combination with cobrotoxin for 1.5 h, which was the time required for induction of NF-κB activation maximally. NF-κB DNA binding activities of nuclear extracts obtained from LPS and cobrotoxin-treated astrocytes (Figure 2Da) and Raw 264.7 cells (Figure 2Db) were much reduced versus the NF-κB DNA binding activity of LPS treated cells in a dose-dependent manner. This effect was observed in astrocytes treated with other stimuli (e.g., SNP-treated astrocytes (Figure 2Dc) and for Raw 264.7 cells also (Figure 2Dd). The specificity of NF-κB DNA binding activity was evidenced either by supershift assay using antibodies for p65 and the p50 component of NF-κB (Figure 3C) or by competition assay versus excessive amounts of unlabeled/cold oligonucleotides and unrelated oligonucleotides (AP-1 and SP-1) in a reaction mixture containing Raw 264.7 cell nuclear extract (Figure 3B,C). A similar pattern of specificity was observed in a reaction mixture containing astrocyte nuclear extract (data not shown).

Inhibition of NF-κB-Dependent Luciferase Activity. Transcriptional regulation is implicated in the expression of genes associated with the NF-κB signaling pathway. To determine the effect of the interaction between cobrotoxin and molecules in the NF-κB signal pathway on NF-κB-dependent gene transcription, we observed NF-κB transcription activity using a transient transfection assay system containing a fusion gene of SV40 promoter, five repeats of the consensus NF-κB binding sequence, and luciferase reporter gene. Astrocytes and Raw 264.7 cells were transfected with this promoter−reporter gene construct, and transcriptional activities were measured after stimulating the cells with SNP or LPS with/without cobrotoxin (Figure 3). Cotreatment of the transfected cells with cobrotoxin (0.1−1 μg/mL range) significantly inhibited the luciferase activity induced by LPS or SNP in astrocytes (by 6−7-fold) (Figure 3A,B) and in Raw 264.7 cells (by 4−10-fold) (Figure 3C,D). These effects suggest that physical the interaction between cobrotoxin and molecules associated with NF-κB signals can change the transcriptional and/or biological effect of NF-κB. Cell viability was measured by WST-1 assay to confirm that the above inhibitory effect of NF-κB was not the result of a toxic effect (i.e., cell death induced by cobrotoxin). Astrocytes (1

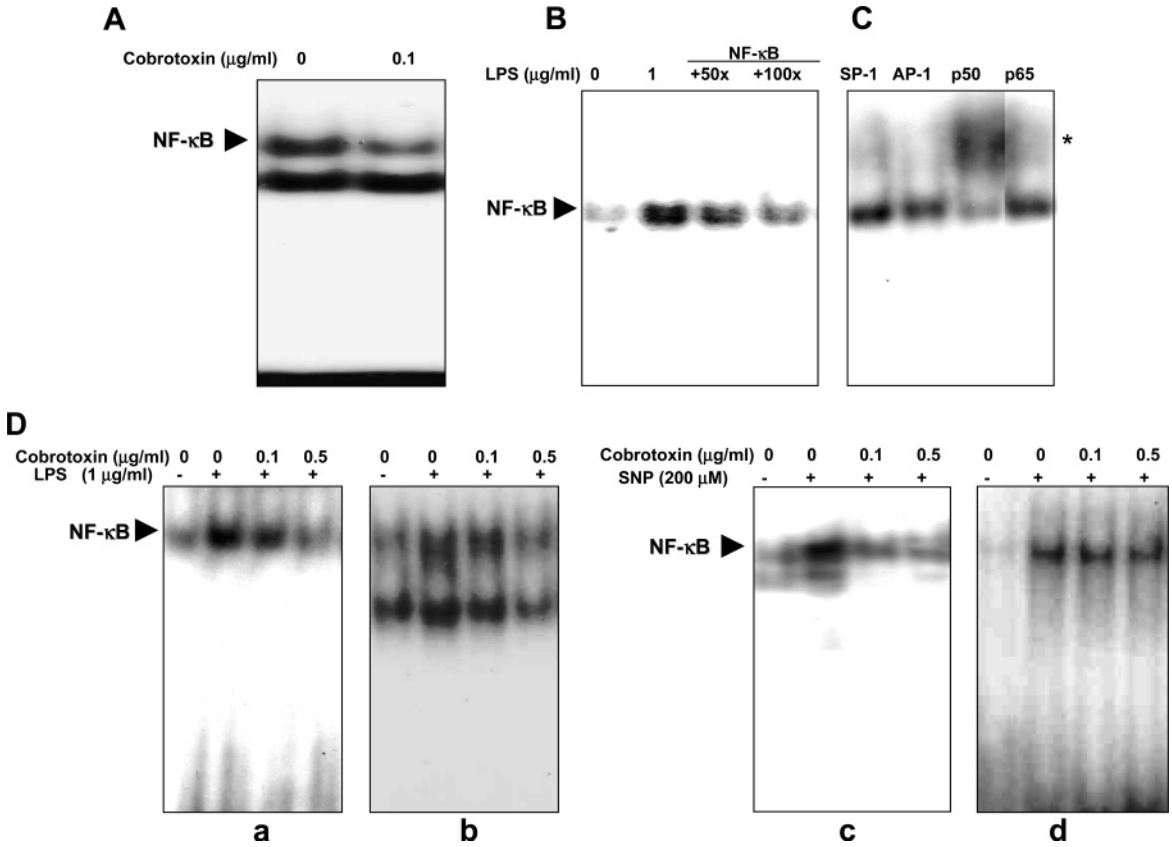

FIGURE 2: Inhibition of NF-κB activation by cobrotoxin. The activation of NF-κB was investigated by EMSA as described in Materials and Methods. (A) p50 from LPS-treated astrocytes was incubated with NF-κB DNA binding element in the absence or presence of cobrotoxin, and then EMSA was performed to determine the binding ability of NF-κB with DNA. (D) Nuclear extracts from astrocytes (a and c) or Raw 264.7 cells (b and d) treated with either LPS (1 μg/mL) or SNP (200 μM) or with cobrotoxin (0.1$\sim$0.5 μg/μL) were incubated with ^{32}P-end-labeled oligonucleotide containing the κB sequence. NF-κB DNA binding activity was determined by EMSA. Each panel is representative of three experiments with triplicates. (C) For supershift assays, nuclear extracts from cells treated with LPS (1 μg/mL) were incubated with specific Abs against p50 and p65 NF-κB isoforms for 1 h before EMSA. ★, supershift by p50 antibody. (B) For competition assays, nuclear extracts from raw 264.7 cells treated with LPS (1 μg/mL) were incubated with unlabeled NF-κB (100$\times$ and 200$\times$) or labeled SP-1 (100$\times$) and AP-1 (100$\times$) for 1 h before EMSA.

$\times 10^5$) were plated into a 96 well plate and then were treated with several concentrations (0.1$\sim$5 μg/mL) of cobrotoxin at 37 °C for 24 h. The cells were then treated with WST-1 for 4 h, and optical densities were read at 450 nm. The presence of cobrotoxin at 0.1$-$1 μg/mL actually increased cell survival in a dose-dependent manner through this concentration range, though survival was significantly reduced at concentration $>$10 μg/mL (data not shown). Similarly, concentrations of cobrotoxin (up to 5 μg/mL) had no cytotoxic effect on Raw 264.7 cells (data not shown).

Inhibitory Effect of Cobrotoxin on the Expression of NF-κB Target Genes. The inhibition of NF-κB could influence the expression of genes regulated by NF-κB. Thus, we examined whether cobrotoxin inhibits the SNP or LPS-induced expression of COX-2, cPLA$_2$, iNOS, IL-4, or TNF-α protein, which are known to be regulated by NF-κB, and which are implicated in inflammatory reaction and cell survival. These proteins were found to be maximally expressed at 24 h after LPS treatment in astrocytes and Raw 264.7 cells (data not shown). Therefore, the expression patterns of the above species were examined at 24 h after cobrotoxin treatment. LPS-induced COX-2, cPLA$_2$, iNOS, and TNF-α protein expressions in astrocytes were found to be dose dependently inhibited by cobrotoxin in agreement with the reducing effect on the activity of NF-κB in both cells types (Figure 4A). These inhibitory effects were also confirmed by examining the expression of COX-2 induced by TNF-α, SNP, and LPS in astrocytes (Figure 4B). We also determined the inhibitory effect of cobrotoxin on the expressions of the proteins of the NF-κB subunit. LPS-induced IκB, phosphorylated IκB, and p50 protein expression were dose dependently inhibited by cobrotoxin in astrocytes (Figure 4C) and Raw 264.7 cells (Figure 4D), but LPS-induced p65 protein expression was not inhibited (data not shown). Further confocal microscopic observations demonstrated that cobrotoxin treatment dose dependently delayed and reduced the nuclear translocation of the p50 subunit (Figure 4E), but had no effect on p65 translocation (data not shown).

Cysteine Residues May Be Involved in the Interaction between Cobrotoxin and NF-κB Signaling Molecules. The X-ray analysis has previously defined the presence of cysteine residues in the p50 of DNA-binding domain, and IKKs also contain cysteine residue at their active sites. Several investigations have shown that the disruption of cysteine residues in these molecules can inhibit NF-κB activation (see Discussion). To explore this possibility, an NF-κB DNA binding element mixture was incubated with cobrotoxin in the presence of the disulfide reducing agents, dithiothreitol (DTT) and GSH, and then DNA binding activity was determined by EMSA. DTT and GSH abrogated the inhibitory effect of cobrotoxin on p50 DNA binding ability in astrocytes as induced by LPS and SNP (Figure

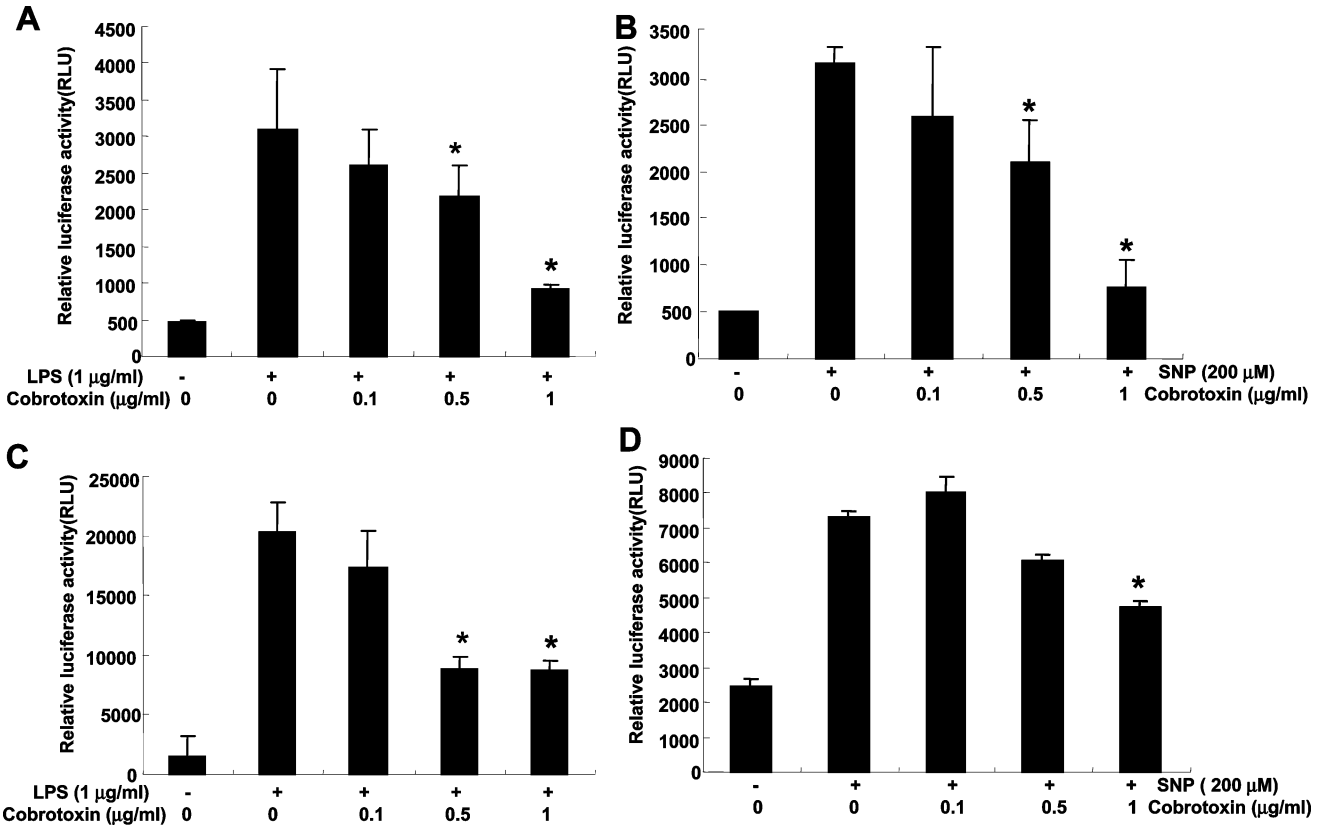

FIGURE 3: Effect of cobrotoxin on LPS- and SNP-induced NF-κB-dependent luciferase activity in astrocytes and Raw 264.7 cells. Astrocytes (A and B) and Raw 264.7 cells (C and D) were transfected with pNF-κB−Luc plasmid (5× NF-κB) and then activated with LPS (1 μg/mL) or SNP (200 μM) in the absence or presence of 0.1−1 μg/mL cobrotoxin for 8 h. Luciferase activity was then determined. Values represent the means ± SE of three independent experiments with triplicate. Fold induction is relative to luciferase activity in transfected unstimulated cells. *P < 0.05 indicates significantly different from the LPS and the SNP treated group.

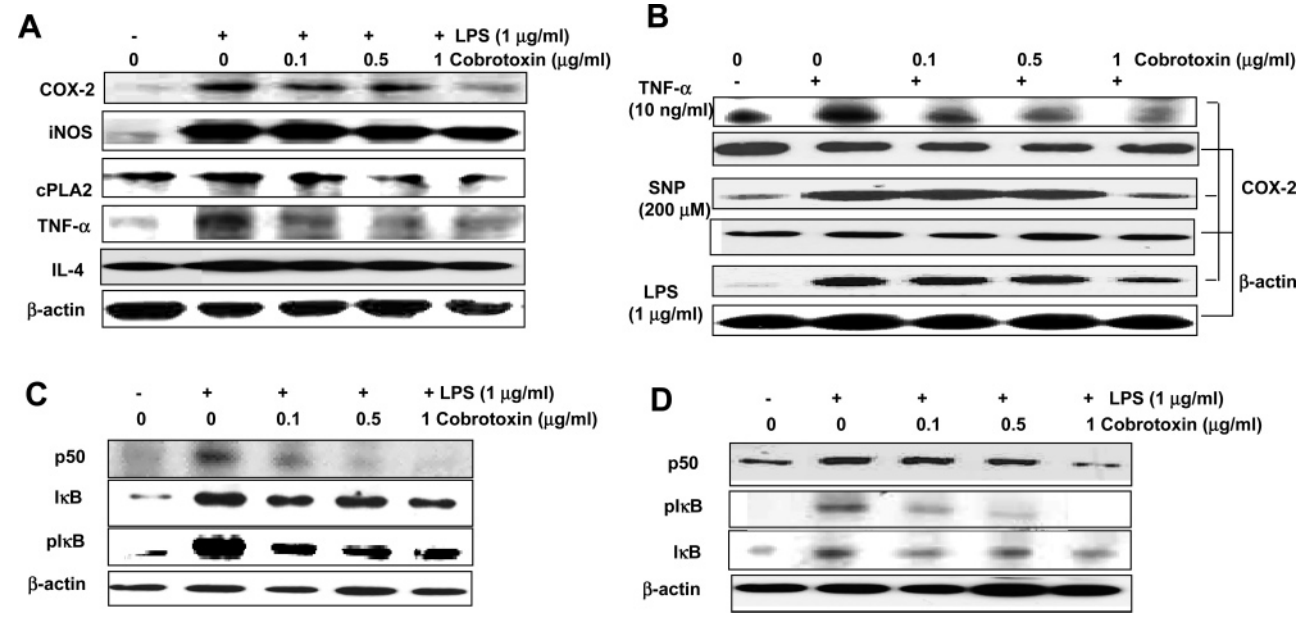

FIGURE 4: Effect of cobrotoxin on LPS-induced inflammatory gene expression in astrocytes. (A) Astrocytes were treated with 0.1−1 μg/mL cobrotoxin in the presence of 1 μg/mL LPS at 37 °C for 24 h. (B) Astrocytes were treated with 0.1−1 μg/mL cobrotoxin in the presence of 1 μg/mL LPS or SNP (200 μM) or TNF-α (1 μg/mL) at 37 °C for 1.5 h. Astrocytes (C) or Raw264.7 cells (D) were treated with 0.1−1 μg/mL cobrotoxin in the presence of 1 μg/mL LPS (1 μg/mL) at 37 °C for 1.5 h. Equal amounts of cytosolic or nucleus proteins (45 μg/lane) were subjected to 10% SDS−PAGE, and then expression of COX-2, iNOS, cPLA$_2$, IL-4, TNF-α proteins (A), COX-2 (B) in the cytosol, and the expression level of p50 in the nucleus and cytosolic IκBα and pIκBα protein (C and D) were detected by Western blotting using specific antibodies. β-actin protein was used as an internal control.

5A). The inhibitory effect of cobrotoxin on DNA binding activity of NF-κB was also abrogated by GSH in Raw 264.7 cells treated with LPS and SNP-treated Raw 264.7 cells (Figure 5B). The results correlate well with the abrogation of NF-κB DNA binding activity. The exogenous addition of DTT and GSH to cells also abrogated the inhibitory effect

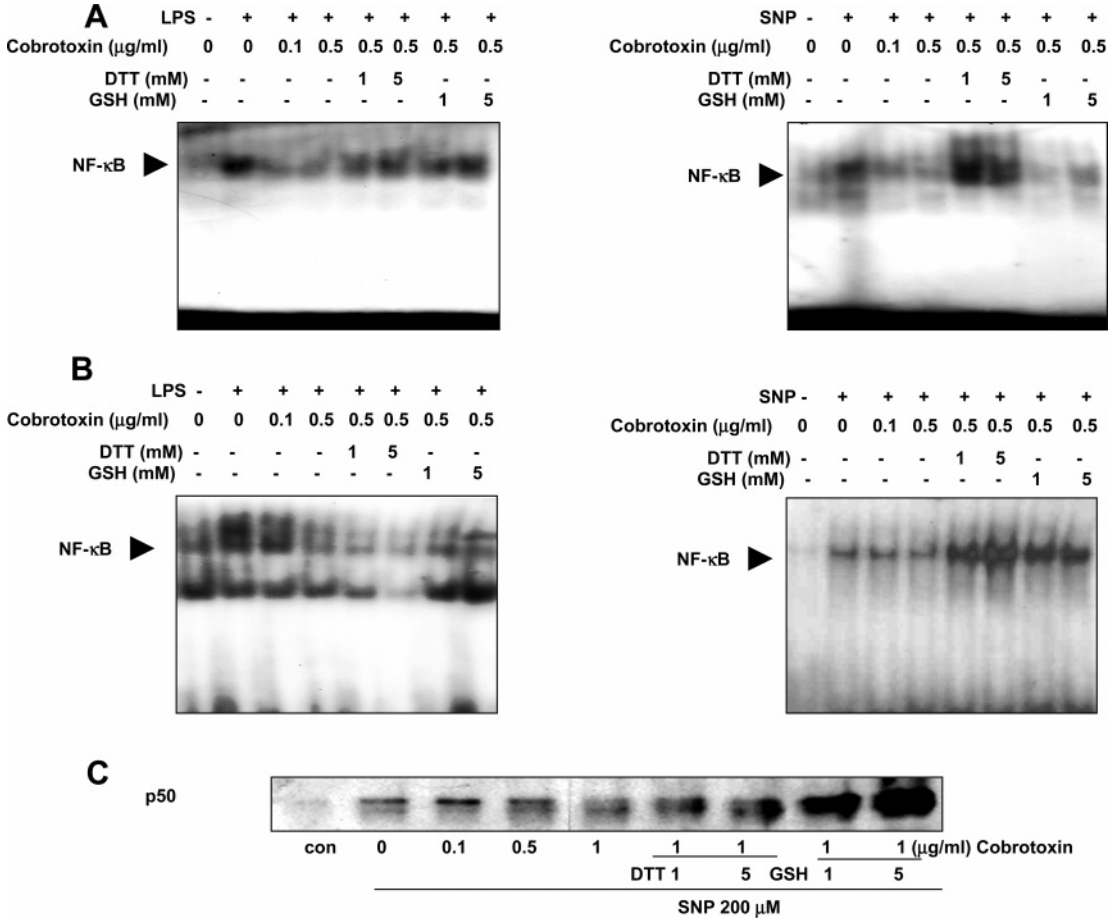

FIGURE 5: The abrogation of the inhibitory effect of cobrotoxin on NF-κB activity induced by LPS and SNP by the reducing agents DTT and GSH. NF-κB DNA binding activity in astrocytes (A) or Raw 264.7 macrophages (B) treated with 0.1−0.5 μg/mL cobrotoxin in the presence of LPS (1 μg/mL) or SNP (200 μM) at 37 °C for 1.5 h. NF-κB DNA binding activity was determined by EMSA in the presence or absence of DTT or GSH. (C) Expression of p50 in nucleus of astrocytes treated with cobrotoxin and SNP in the absence or presence of DDT or GSH. Each panel is representative of two experiments with triplicates.

of cobrotoxin on p50 translocation to the nucleus in cultured astrocytes (Figure 5C).

To further investigate this effect of DTT and GSH on the direct binding of cobrotoxin with p50 and IKKs, surface plasmon resonance analysis was performed. Decreases in the interaction between cobrotoxin and immunoprecipitated p50, IKKα, and IKKβ extracted from cells treated with SNP and cobrotoxin were absent in cells treated with SNP and cobrotoxin in the presence of DTT or GSH (Figure 6). We also conducted a transient transfection assay with a fusion gene containing pCMV promoter and p50 and IKKs mutants. Interestingly, the endogenous DNA binding activity of NF-κB was elevated in astrocytes transfected with mutant of p50 and IKKα, but LPS did not increase further the DNA binding activity of NF-κB. Cotreatment with LPS and cobrotoxin did not inhibit LPS-induced NF-κB activity in astrocytes transfected with p50 (C62S) and IKKα (C178A) mutants (Figure 7A). Astrocytes transfected with IKKβ (C179A) and cobrotoxin did not inhibit LPS-induced NF-κB activity. A similar effect was seen in TNF-α-treated cells (Figure 7B). However, the inhibitory effect of cobrotoxin on inflammatory stimulation was regained by cells transfected with IKKβ mutant (K44A), suggesting that these cysteine residues are target of cobrotoxin.

We also further investigated whether cobrotoxin can be uptaken by cells and thereby interact with NF-κB signal molecules. For this purpose, we labeled cobrotoxin with Alexa Fluor 488, a photostable dye, using a protein labeling kit. Cobrotoxin/Alexa Fluor conjugate was added to astrocytes or RAW264.7 cells, and the uptake of labeled cobrotoxin into the cells was followed under a confocal laser scanning microscope as shown in Figure 8A. Moreover, the uptake of cobrotoxin into the nucleus of Raw 264.7 cells was evidenced by double staining, that is, a merge of the PI staining and the labeled cobrotoxin located in the nucleus as shown in the Figure 8B. Figure 8C shows a negative control of uptake of cobrotoxin in the presence of 1 mM sodium azide.

DISCUSSION

The present study demonstrates that cobrotoxin binds to the molecules in the NF-κB signaling pathway with high affinity. The binding affinity of cobrotoxin to IKKα was 2.16 $\times$ 10^{-9} M (K_d), to IKKβ 3.24 $\times$ 10^{-8} M (K_d), and to p50 1.54 $\times$ 10^{-5} M (K_d). Interaction between cobrotoxin and these NF-κB signaling molecules resulted in the inhibition of DNA binding activities and in the transcriptional activity of NF-κB, thus suppressing the expression of NF-κB target genes such as COX-2, iNOS, $cPLA_2$, IL-4, and TNF-α in addition to suppressing IκB release and p50 translocation. Using reducing agents and transfection assays with plasmids

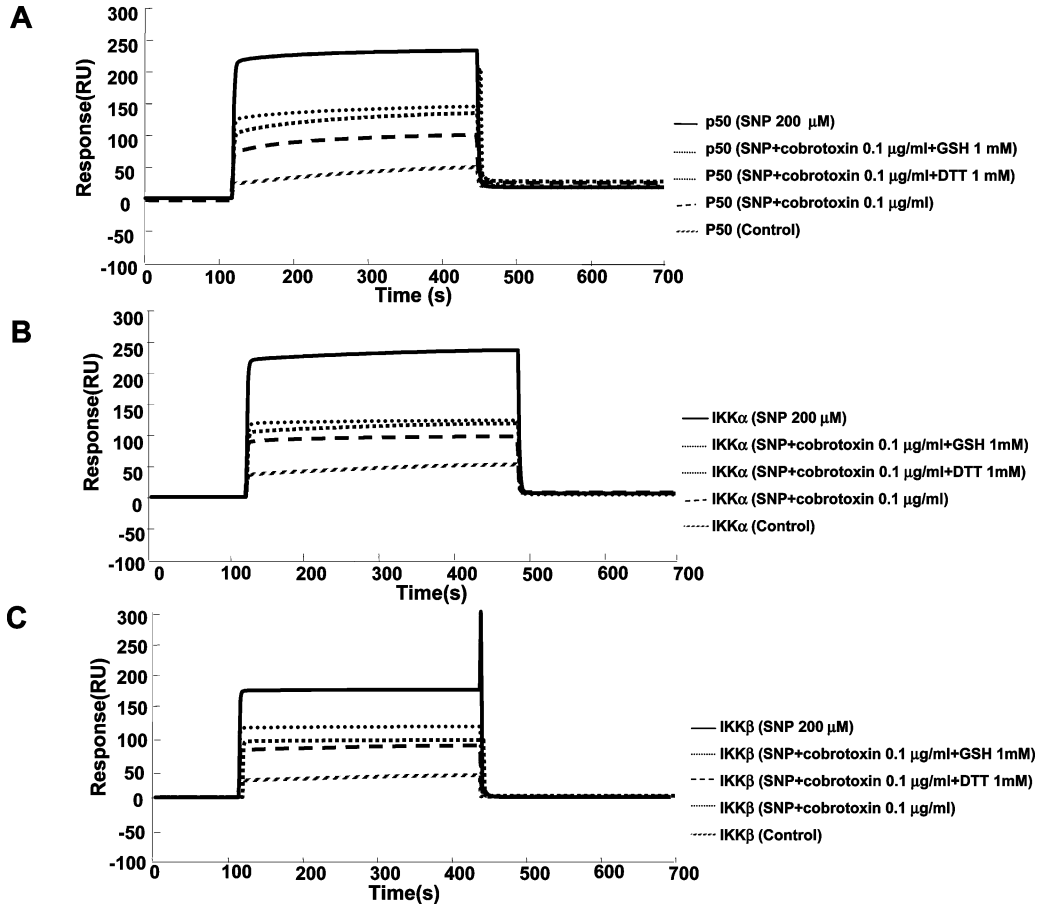

FIGURE 6: Abrogation of cobrotoxin binding affinity for NF-κB signaling molecules by the reducing agents DTT and GSH. Immunoprecipitated NF-κB signal molecules (p50, IKKα, and IKKβ) extracted from each treated astrocytes were flowed through a cobrotoxin immobilized chip as described in Materials and Method. Each line is representative of surface plasmon resonance binding kinetic traces obtained from duplicate experiments. (A−C) Full kinetic dataset of the binding between each NF-κB signaling molecules and immobilized cobrotoxin. Each line represents a 1:1 binding model of the injected group indicated.

containing mutant forms of NF-κB signal molecules (whereby cystein residues were replaced by other amino acids), we found that cobrotoxin probably interacts with the cystein residues of active sites in these molecules.

Cobrotoxin has 12 cystein residues and forms six disulfide bonds. Structural and other studies have shown binding between cobrotoxin and biological receptors such as AchR (*16*−*20*); thus here, we investigated whether cobrotoxin binds to cysteine residues in different target molecules involved in NF-κB signaling such as p50, IKKα, and IKKβ. Although we did not identify the precise binding site, our binding affinity data demonstrate that cobrotoxin binds to p50 and IKKs with high affinity, and we determined cobrotoxin binding affinities to IKKα ($K_d = 2.16 \times 10^{-9}$ M), IKKβ ($K_d = 3.24 \times 10^{-8}$ M), and p50 ($K_d = 1.54 \times 10^{-5}$ M). These binding affinities of cobrotoxin to IKKs are comparable to its binding affinity to nicotinic AchR ($K_d = (1-12) \times 10^{-9}$ M, *16*). Moreover, this strong binding of cobrotoxin to IKKs is likely to change or reduce their activities and markedly reduce NF-κB activation. Taking this perspective, we demonstrated the inhibitory effect of cobrotoxin on the DNA binding activity of NF-κB in vivo and in vitro (cell free system) and on the transcriptional activities of NF-κB and on the expression of NF-κB target genes involved in inflammatory responses and cancer development, that is, COX-2, $cPLA_2$, iNOS, IL-4, and TNF-α in astrocytes and in Raw 264.7 cells induced by LPS and SNP. These data suggest that the binding of cobrotoxin to NF-κB signal molecules alter the NF-κB signaling pathway and indicate that small amounts of cobrotoxin may be used therapeutically to control pathophysiological conditions such as inflammatory reactions and cancer development. In fact, the binding affinities of IKKα, IKKβ, and p50 proteins (immunoprecipitates from the LPS-treated cells against anti IKKα, IKKβ, and p50 antibodies) with cobrotoxin immobilized on a sensor protein chip was much lower in cells treated with LPS in combination of cobrotoxin than in cells treated with LPS alone. The concentrations of cobrotoxin used in the present study were not cytotoxic to astrocytes or Raw 264.7 cells even in the presence of inflammatory inducers. In addition, it was found that pico- or nanomolar concentrations of cobrotoxin can induce apoptotic cell death and the expression of genes related to cell survival in the prostate cancer cell lines PC-3 and LNCaP (unpublished data). It is noteworthy that Utkin et al. suggested the pharmacological importance of the antagonistic effect of "weak toxin" from *Naja kaouthia* snake venom toxin to AchRs (*25*).

We also identified possible sites in NF-κB molecules reactive to cobrotoxin. Structural IKKs and p50 subunit data have revealed that cysteine residues are present in the catalytic domain of IKKα and IKKβ and in the DNA binding domain of p50. On the basis of structural data, several studies have demonstrated that the cysteine residues of these molecules are targeted by compounds that can inhibit NF-

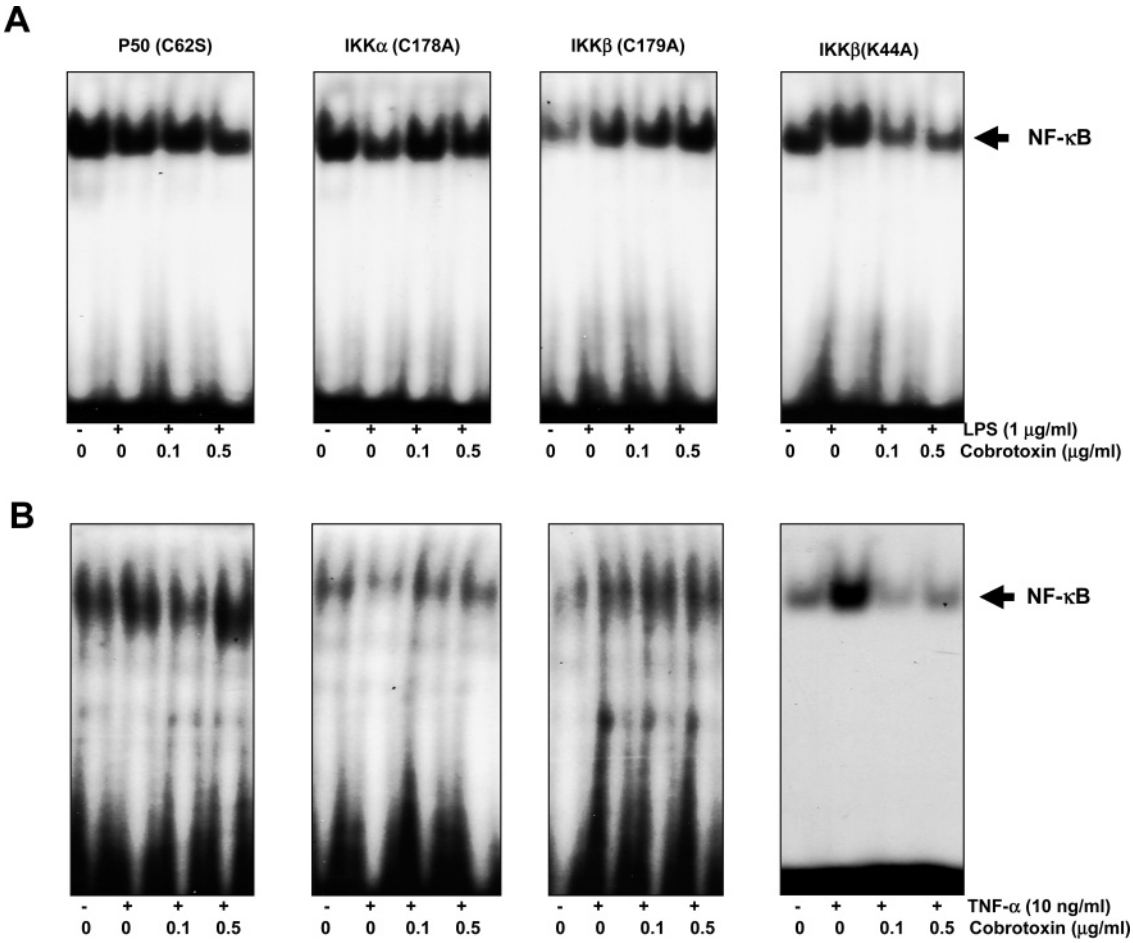

FIGURE 7: Abolition of the inhibitory effect of cobrotoxin on NF-κB activity. Astrocytes were transfected with mutant p50 (C62S), IKKα (C178A), and IKKβ (C179A) or IKKβ (K44A) mutant plasmid and then treated with LPS (1 μg/mL, A) or TNF-α (10 ng/mL, B) with/without 0.1−0.5 μg/mL of cobrotoxin at 37 °C for 24 h. NF-κB DNA binding activity was determined by EMSA. Each panel is representative of two similar experiments performed in triplicates.

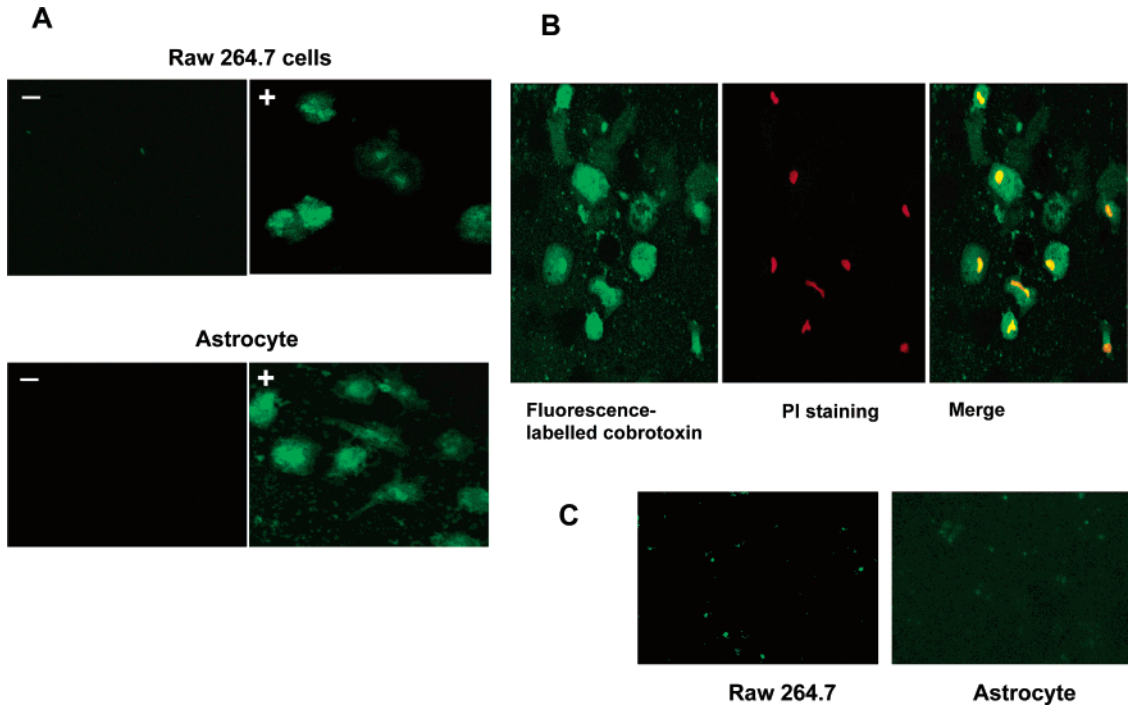

FIGURE 8: Uptake of cobrotoxin by cells. (A) Cobrotoxin uptake into the cytosol and nucleus of Raw 264.7 cells or astrocytes as demonstrated by confocal laser scanning microscopy (×360). Negative (−), cells were treated with unlabeled cobrotoxin, and nuclei were stained with PI. Positive (+), cells were treated with cobrotoxin labeled with Alexa Fluor 488 dye. (B) Double staining (merge) with labeled cobrotoxin by PI staining demonstrating the localization of cobrotoxin in the nucleus. (C) Uptake of cobrotoxin labeled with Alexa Fluor 488 dye in the presence of 1 mM sodium azide.

κB activity. For example, kamebakaurin and other three kaurane diterpenes in the extract of *Isodon japonicus* selectively inhibit the activation of NF-κB by directly interacting with the cysteine residues of p50 (*7*). In another report, the synthetic quinone derivative, (2*E*)-3-[5-(2,3-dimethoxy-6-methyl-1, 4-benzoquinoyl)]-2-nonyl-2-propenoic acid (E3330), a novel anti-NF-κB drug, was found to specifically suppress the DNA binding activity of NF-κB by interacting with the cysteine residue of p50 (*22*). The mercuric ion (Hg^{2+}), a potent thiol inhibitor, also prevents the expression of NF-κB by mercaptide bond formation with the p50 subunit (*23*). It has also been shown that natural compounds and other thiol bonding metals inhibit NF-κB activation by interacting with the cysteine residue of the IKK catalytic subunits (*5*, *6*). We also recently found that melittin, a cationic 26-amino acid compound and the principal active component of bee venom toxin, and bee venom itself, directly bind to the sulfhydryl group of p50 to reduce IκB release and/or p50 translocation, and thereby inhibit the activation of NF-κB and the expression of genes regulated by NF-κB (*21*). In the present study, the exogenous addition of the thiol reducing agents, DTT and GSH, reversed the binding affinity of cobrotoxin to p50, IKKα, and IKK*β* and also abrogated the inhibitory effect of cobrotoxin on p50 DNA binding activity and transcription activities. This result is in agreement with other data that the cysteine residue may be targeted by compounds that inhibit NF-κB (*25*−*27*). These data therefore suggest that cobrotoxin modifies the sulfhydryl group in IKKα, IKK*β*, and p50 proteins. This notion was further reinforced by our finding that the inhibitory effect of cobrotoxin on SNP or LPS-induced NF-κB activity was abolished in cells transfected with p50, IKKα, or IKK*β* mutant plasmids, in which cysteine residues in active sites were replaced by other amino acids. A similar effect was reported for the peroxisome proliferators activated receptor gamma agonist 15-deoxy-delta12, 14-prostaglandin J_2 (15-deoxy PGJ_2) which inhibited IκBα degradation by covalent modifying IKKα and IKK*β* through a Michael-type reaction (*9*). In another study, arsenite, a potent inhibitor of NF-κB activation, was shown to interact with a specific cysteine residue (Cys-179) of the IKK catalytic subunit, and this interaction was found to be inhibited by thiol-modifying agents (*6*). This thiol redox mechanism was also found to be involved in the metal (gold)-induced inhibition of IKKs (*27*). It is interesting to note that the binding affinity of cobrotoxin for AchR was negated by DTT (reducing agent) and 2,2-dihydropyridine (a cysteine modifying agent) (*20*). Taken together, the present results show that cobrotoxin binds to p50, IKKα, and IKK*β* probably via cysteine residues. This binding could inhibit the expressions of NF-κB target genes by inhibiting p50 translocation either by direct binding to p50 or by inhibiting IKKα and IKK*β* activation in the cytosol. The direct inhibition of the DNA binding activity of NF-κB in the nucleus is also a possibility since cobrotoxin was found to be uptaken by the nucleus. The identification of cobrotoxin binding sites and the involvement of disulfide bonds in the binding between cobrotoxin and NF-κB signaling molecules are being investigated. In summary, the present results demonstrate that cobrotoxin directly binds to the sulfhydryl group of p50 and IKKs, which reduces p50 translocation and IκB release, and thereby inhibits NF-κB activation. Our data suggest that pico- to nanomolar concentrations of cobrotoxin may be useful in the treatment of cancer and inflammatory diseases.

REFERENCES

1. Li, Q., and Verma, I. M. (2002) NF-kappaB regulation in the immune system, *Nat. Rev. Immunol. 10*, 725−734.
2. Burstein, E., and Duckett, C. S. (2003) Dying for NF-kappaB? Control of cell death by transcriptional regulation of the apoptotic machinery, *Curr. Opin. Cell Biol. 6*, 732−737.
3. Karin, M., and Delhase, M. (2000) The I kappa B kinase (IKK) and NF-kappa B: key elements of proinflammatory signaling, *Semin. Immunol. 1*, 85−98.
4. Karin, M. (1999) The beginning of the end: IkappaB kinase (IKK) and NF-kappaB activation, *J. Biol. Chem. 39*, 27339−27342.
5. Jeon, K. I., Byun, M. S., and Jue, D. M. (2003) Gold compound auranofin inhibits IkappaB kinase (IKK) by modifying Cys-179 of IKKbeta subunit, *Exp. Mol. Med. 2*, 61−66.
6. Kapahi, P., Takahashi, T., Natoli, G., Adams, S. R., Chen, Y., Tsien, R. Y., and Karin, M. (2000) Inhibition of NF-kappa B activation by arsenite through reaction with a critical cysteine in the activation loop of Ikappa B kinase, *J. Biol. Chem. 46*, 36062−36066.
7. Lee, J. H., Koo, T. H., Hwang, B. Y., and Lee, J. J. (2002) Kaurane diterpene, kamebakaurin, inhibits NF-kappa B by directly targeting the DNA-binding activity of p50 and blocks the expression of antiapoptotic NF-kappa B target genes, *J. Biol. Chem. 21*, 18411−18420.
8. Xia, Y. F., Ye, B. Q., Li, Y. D., Wang, J. G., He, X. J., Lin, X., Yao, X., Ma, D., Slungaard, A., Hebbel, R. P., Key, N. S., and Geng, J. G. (2004) Andrographolide attenuates inflammation by inhibition of NF-kappa B activation through covalent modification of reduced cysteine 62 of p50, *J. Immunol. 173*, 4207−4217.
9. Straus, D. S., Pascual, G., Li, M., Welch, J. S., Ricote, M., Hsiang, C. H., Sengchanthalangsy, L. L., Ghosh, G., and Glass, C. K. (2000) 15-Deoxy-$\Delta^{12,14}$-prostaglandin J_2 inhibits multiple steps in the NF-κB signaling pathway, *Proc. Natl. Acad. Sci. U.S.A. 97*, 4844−4849.
10. Samson, A., Scherf, T., Eisenstein, M., Chill, H. J., and Anglister, J. (2002). The mechanism for acetylcholine receptor inhibition by alpha-neurotoxins and species-specific resistance to alpha-bungarotoxin revealed by NMR, *Neuron 35*, 319−332.
11. Sher, E., Giovannini, F., Boot, J., and Lang, B. (2000) Peptide neurotoxins, small-cell lung carcinoma andneurological paraneoplastic syndromes, *Biochimie 82*, 927−936.
12. Van Lutern, E., and Moyer, M. (1999) Peptide toxin blockers of voltage-sensitive K+ channels: inotropic effects on diaphragm, *J. Appl. Physiol. 3*, 1009−1016.
13. Brown, R. L., Haley, T. L., West, K. A., and Crabb, J. W. (1999) Pseudechetoxin: a peptide blocker of cyclic nucleotide-gated ion channels, *Proc. Natl. Acad. Sci. U.S.A. 96*, 754−759.
14. Hopkins, W. F. (1998) Toxin and subunit specificity of blocking affinity of three peptide toxins for heteromultimeric, voltage-gated potassium channels expressed in Xenopus oocytes, *J. Pharmacol. Exp. Ther. 3*, 1051−1060.
15. Siigur, E., Aaspollu, A., and Siigur, J. (2001) Sequence diversity of *Vipera lebetina* snake venom gland serine proteinase homologs—result of alternative-splicing or genome alteration, *Gene 263*, 199−203.
16. Servent, D., Winckler-Dietrich, V., Hu, H. Y., Kessler, P., Drevet, P., Bertrand, D., and Menez, A. (1997) Only snake curaremimetic toxins with a fifth disulfide bond have high affinity for the neuronal alpha7 nicotinic receptor, *J. Biol. Chem. 39*, 24279−24286.
17. Conroy, W. G., Saedi, M. S., and Lindstrom, J. (1990) TE671 cells express an abundance of a partially mature acetylcholine receptor alpha subunit which has characteristics of an assembly intermediate, *J. Biol. Chem. 35*, 21642−21651.
18. Michalet, S., Teixeira, F., Gilquin, B., Mourier, G., Servent, D., Drevet, P., Binder, P., Tzartos, S., Menez, A., and Kessler, P. (2000) Relative spatial position of a snake neurotoxin and the reduced disulfide bond alpha (Cys192−Cys193) at the alpha gamma interface of the nicotinic acetylcholine receptor, *J. Biol. Chem. 33*, 25608−25615.
19. Kachalsky, S. G., Jensen, B. S., Barchan, D., and Fuchs, S. (1995) Two subsites in the binding domain of the acetylcholine receptor: an aromatic subsite and a proline subsite, *Proc. Natl. Acad. Sci. U.S.A. 92*, 10801−10805.

20. McLaughlin, J. T., Hawrot, E., and Yellen, G. (1995) Covalent modification of engineered cysteines in the nicotinic acetylcholine receptor agonist-binding domain inhibits receptor activation, *Biochem. J. 15*, 765−769.
21. Park, H. J., Lee, S. H., Son, D. J., Oh, K. W., Kim, K. H., Song, H. S., Kim, G. J., Oh, G. T., Yoon, D. Y., and Hong, J. T. (2004) Antiarthritic effect of bee venom: inhibition of inflammation mediator generation by suppression of NF-kappaB through interaction with the p50 subunit, *Arthritis Rheum. 50*, 3504−3515.
22. Goto, M., Yamada, K., Katayama, K., and Tanaka, I. (1996) Inhibitory effect of E3330, a novel quinone derivative able to suppress tumor necrosis factor-alpha generation, on activation of nuclear factor-kappa B, *Mol. Pharmacol. 49*, 860−873.
23. Dieguez-Acuna, F. J., and Woods, J. S. (2000) Inhibition of NF-kappaB-DNA binding by mercuric ion: utility of the non-thiol reductant, tris(2-carboxyethyl)phosphine hydrochloride (TCEP), on detection of impaired NF-kappaB-DNA binding by thiol-directed agents, *Toxicol. in Vitro 14*, 7−16.
24. Utkin, Y. N., Kukhtina, V. V., Kryukova, E. V., Chiodini, F., Bertrand, D., Methfessel, C., and Tsetlin, V. I. (2000) "Weak toxin" from *Naja kaouthia* is a nontoxic antagonist of alpha 7 and muscle-type nicotinic acetylcholine receptors, *J. Biol. Chem. 276*, 15810−15815.
25. Garcia-Pineres, A. J., Castro, V., Mora, G., Schmidt, T. J., Strunck, E., Pahl, H. L., and Merfort, I. (2001) Cysteine 38 in p65/NF-kappaB plays a crucial role in DNA binding inhibition by sesquiterpene lactones, *J. Biol. Chem. 276*, 13−20.
26. Kim, I. Y., and Stadtman, T. C. (1997) Inhibition of NF-kappaB DNA binding and nitric oxide induction in human T cells and lung adenocarcinoma cells by selenite treatment, *Proc. Natl. Acad. Sci. U.S.A. 94*, 12904−12907.
27. Jeon, K. I., Jeong, J. Y., and Jue, D. M. (2000) Thiol-reactive metal compounds inhibit NF-kappa B activation by blocking I kappa B kinase, *J. Immunol. 11*, 5981−5989.

BI050156H